Lab on a Chip

Accepted Manuscript

ROYAL SOCIETY OF CHEMISTRY

www.rsc.org/loc

Microfluidic Co-Cultures with Hydrogel-Based Ligand Trap to Study Paracrine Signals Giving Rise to Cancer Drug Resistance

Authors:

Dipali Patel [a], Yandong Gao [a*], Kyungjin Son [a], Christian Siltanen [a], Richard M. Neve [b], Katherine Ferrara [a], Alexander Revzin [a,*]

Affiliation:

[a] *Department of Biomedical Engineering, One Shields Ave., University of California, Davis, CA, 95618*

[b] *Department of Discovery Oncology, Genentech Inc., 1 DNA Way, South San Francisco, CA, 94080, USA.*

Corresponding author: arevzin@ucdavis.edu, ydgao@ucdavis.edu

Abstract

Targeted cancer therapies are designed to deactivate signaling pathways used by cancer cells for survival. However, cancer cells are often able to adapt by activating alternative survival pathways, thereby acquiring resistance to such drugs. An emerging theory is that autocrine or paracrine growth factors in the cancer microenvironment are one mechanism through which this is achieved. In the present study we wanted to examine whether paracrine interactions between groups of melanoma cells result in resistance to vemurafenib – an FDA approved drug targeting the *BRAF* mutation in metastatic melanoma. We used a vemurafenib-resistant melanoma model which secretes fibroblast growth factor (FGF)-2 to test our hypothesis that this is a key paracrine mediator of resistance to vemurafenib. Sensitive cells treated with media conditioned by resistant cells did not protect from the effects of vemurafenib. To query paracrine interactions further we fabricated a microfluidic co-culture device with two parallel compartments, separated by a 100 μm wide hydrogel barrier. The gel barrier prevented resorting/contact of cells while permitting paracrine cross-talk. In this microfluidic system, sensitive cells did become refractive to the effects of vemurafenib when cultured adjacent to resistant cells. Importantly, incorporation of anti-FGF-2 antibodies into the gel barrier separating the two cell types prevented onset of resistance to vemurafenib. Microfluidic tools described here allow for more sensitive analysis of paracrine signals, may help better understand signaling in the cancer microenvironment and may enable development of more effective cancer therapies.

INTRODUCTION

Increased understanding of molecular mechanisms and genes associated with cancer cell survival has led to the development of therapies targeting pro-survival mechanisms. Vemurafenib is one example of pathway-targeted drug used treat patients with metastatic melanoma.[1] This drug is designed to target *BRAF* mutant melanomas and acts by inhibiting mutant BRAF – a kinase which activate the mitogen-activated protein kinase (MAPK) pathway – thereby preventing downstream signaling associated with cell survival.[1-3] Vemurafenib is effective initially,[4, 5] however, patients become refractive to the treatment several months later.[6] The acquired drug resistance is not unique to vemurafenib; it is in fact a tremendous problem that undermines effectiveness of most targeted therapeutics.[7-10]

What causes drug resistance? There is considerable evidence to suggest that growth factors produced in the cancer microenvironment condition cancer cells to activate alternative survival pathways circumventing those being blocked by targeted therapies.[7, 8, 11] Interestingly, drug resistance need not be the result of complex signaling cascade by multiple growth factors (GFs). For example, recent work by two groups pointed to HGF as a possible reason for resistance in glioblastoma, melanoma and colorectal cancer cell lines containing *BRAF* mutation.[8, 12] In these studies, a combination of vemurafenib and inhibitor of HGF receptor (c-met) was shown to significantly improve effectiveness of therapy. Therefore, understanding how GFs contribute to drug resistance may be leveraged towards developing combination therapies with improved cancer-killing effectiveness.

Where do resistance-causing GFs originate from? The cellular origins of resistance-causing GFs are not well understood, with contributions from stroma[12] or a subpopulation of naturally resistant cancer cells being considered as possibilities.[13, 14] Furthermore, there is evidence of complex reciprocal interactions whereby drug-sensitive cancer cells may be secreting factors that enhance survival and proliferation of the drug-resistant cells.[15] These past studies underscore the importance of cellular cross-talk and paracrine signaling in the context of cancer microenvironment. Herein, we wanted to develop a

sensitive cell culture platform in order to study the role of paracrine signals in conferring drug resistance. The focus of our studies was on fibroblast growth factor (FGF)-2 mediated resistance of *BRAF* mutant melanoma cells to treatment with BRAF inhibitor vemurafenib. FGF-2 is an important protein involved in a range of processes from embryonic development to cancer metastasis.[16] FGF-2 has been implicated in improving cancer cell survival during anti-cancer drug therapy.[17, 18] and is secreted in response to vemurafenib treatement.[19] Particularly, we wanted to test the hypothesis that cell-secreted FGF-2 plays a key role in activating alternative survival pathways in melanoma cells.

The standard methods for dissecting exchange of paracrine signals between groups of cells include transwell cultures and conditioned media experiments. However, these culture techniques utilize large volumes of media and likely dilute important secreted molecules below threshold levels required for activating signaling pathways. In addition, local concentration gradients are destroyed with conditioned media experiments.[20] Placing the cells in close proximity on the culture surface is likely more optimal from the standpoint of preserving high (physiological) concentrations of secreted GFs. Micropatterned co-cultures offer one option for placing two cell types into close proximity to each other.[21-23] This strategy has worked well for scenarios where the two cell types comprising the co-cultures have distinctly different adhesive properties (e.g. hepatocytes and fibroblasts),[24] however, it is challenging to implement for seeding cells with similar adhesion behavior. An alternative to micropatterned co-cultures is microfluidic co-cultures whereby cells are seeded into adjacent microfluidic chambers and are allowed to communicate by paracrine signals. This communication may occur either via grooves fabricated in the wall separating the adjacent compartments or by means of a retractable wall – a valve raised or lowered by actuating control layer in the microfluidic device.[25-28] Such a microfluidic device allows to co-culture cells with very similar adhesive behavior and also enables selective treatment of the desired cellular compartment with pharmacological agents. For example, we recently employed a microfluidic co-culture system to investigate HGF-mediated paracrine signaling between groups of hepatocytes.[28] However, in the present study we were faced with the fact that melanoma cells were highly migratory and tended to

resort after seeding into adjacent microfluidic compartments. To address this challenge, we incorporated a poly(ethylene glycol) (PEG) hydrogel barrier into a narrow channel separating the cancer cell compartments (Fig. 1(A,B)). This gel not only prevented resorting of cells but could also be converted into a ligand trap to retain a specific paracrine signal of interest while allowing other signals to diffuse from one compartment to the other. Using microfluidic devices with integrated hydrogel barriers we were able to prove that resistant cells secreted FGF-2 which diffused over and made sensitive cells refractive to vemurafenib. Importantly, incorporation of FGF-2 capture probes (Fc-FGFR1 chimera) into the gel barrier separating resistant and sensitive melanoma cells abrogated resistance to vemurafenib. Overall, the microfluidic platform described here offers a new means of investigating paracrine cross-talk in the context of cancer or other diseases.

MATERIALS AND METHODS

Chemicals and materials

Glass slides (75 × 25 mm^2) were obtained from VWR (West Chester, PA). Poly(dimethylsiloxane) (PDMS) was acquired from Dow Corning (Midland, MI). ELISA kit for FGF-2 was purchased from R&D Systems. Phosphate-buffered saline (1× PBS), RPMI-1640, Penicillin Streptomycin, DAPI stain, Live/Dead viability kit and fetal bovine serum (FBS) were purchased from Life technologies. NVP-BGJ398 (FGFR inhibitor) and PD0325901 (MEK inhibitor) were acquired from SelleckChem. Collagen type I was purchased from Corning. Melanoma cells (LOX-IMVI – drug sensitive, LOX-IMVI-R – drug resistant) were used in collaboration with Genentech (San Francisco, CA), A-375 cells were purchased from ATCC (Manassas, VA). PLX4720 (BRAF inhibitor, commercial name vemurafenib) and an FGF-trap – a fusion protein comprised of an Fc domain of an antibody and FGFR1 extracellular domain (Fc-FGFR1) - were a gift from Genentech.

Fabrication of microfluidic devices

The two-layer microfluidic cell culture platform was fabricated using standard soft-lithography techniques and replica molding of PDMS (Ellsworth Adhesives, Germantown, WI). The bottom layer

comprised of 10 μm high grooves that separated PEG chamber from cell culture chambers. The top layer was comprised of two adjacent microchambers (of the dimension 8×1.8×0.075 mm (length×width×height)), separated by a narrow channel (width of 100 μm). The mold for the first layer of PDMS was made by a two-layer fabrication technique. Briefly SU8 2010 first formed a 10 μm high rectangular slab on a silicon wafer. SU8 2050 was then spin-coated to define the mold for the 75 μm high chambers and channels. PDMS base and its curing agent were mixed in a ratio of 10:1 and poured onto the molds in a petri dish. The dish was degassed for 1 hour before being incubated for 2 hours at 70 °C for curing. After the solidified PDMS layers were peeled from its mold, a sharp metal puncher was used to generate holes for inlets and outlets. The first and second PDMS layers were bonded together after both surfaces were treated with oxygen plasma. Subsequently, the PDMS piece was placed on top of a glass slide with imprinted protein spots to complete the device. Four cloning cylinders (Fisher Scientific, Pittsburgh, PA) were attached to the loading wells as reservoirs for culture media and two microbore tubes (Cole-Parmer, Vermon Hills, IL) were attached to the control chamber by gluing with liquid PDMS. The microfluidic device was then sterilized under UV light in a tissue culture hood for 1-2 h before it was ready to culture cells.

To make the gel barrier, a mixture of 5% w/v of 6kDa polyethelene glycol-diacrylate and 1% w/v photoinitiator solution were diluted in PBS and thoroughly vortexed. The solution was infused into the center chamber and the microfluidic device was placed in a nitrogen bag before being exposed to 365 nm, 18W/cm^2 UV light using an OmniCure series 1000 light source (EXFO; Vanier, Quebec, Canada).

Cultivation of cancer cells in microfluidic devices

After fabrication of PEG gel in the middle chamber, the cell culture chambers were infused with 0.2 mg/mL collagen type I and incubated at room temperature for 1 hour. The channels were subsequently rinsed with media before a cell suspension at 1.0×10^6 cells/mL were introduced to the inlets to induce passive flow. After 15 minutes of incubation at 37 °C, the inlets were rinsed twice to detach any cells bound there. Fresh media (450 μL per inlet) was then added and changed daily subsequently.

Live/dead staining

Samples for live/dead cell analysis were stained using manufacturer's instructions (Live/dead cell viability kit, Life Technologies). Briefly, cells were treated with PBS containing 4 μM ethidium homodimer and 2 μM calcein AM for 30 mins at 37 °C. The samples were then rinsed with fresh PBS before being imaged. ImageJ software was used to quantify numbers of live (green) and dead (red) cells to generate %viability data.

FGF-2 ELISA

The cell media was collected from microfluidic channel outlets every 24 h. After 48 hours of culture, media from both time points were mixed together and the cumulative FGF-2 released by cells was quantified as per the manufacturer's instructions (R&D Systems). For each condition, samples were acquired from three independent microfluidic devices. Each sample was run in triplicate on an ELISA plate.

Viability and proliferation analysis

MTT Assay: Cell proliferation assay was conducted according to manufacturer's instructions (Life Technologies). Briefly, a final concentration of 0.5mg/ml MTT solution (diluted in serum-free RPMI) was added to each well in a 96-well plate and incubated for 4 hours at 37C. After incubation, MTT solution was aspirated and discarded and 100 ul DMSO was added to each well. Absorbance was read at 570 nm.

Live/Dead staining: Cell viability was assayed using manufacturer's instructions (Life technologies). Briefly, cells were quickly washed with PBS first. They were then treated with a cocktail solution of 2 μM calcein AM and 4 μM EthD-1 solution in PBS. Following a 20 minute incubation at 37C, the cells were washed with PBS again and imaged immediately using an inverted fluorescence microscope. ImageJ software was used to quantify cell numbers.

Modeling secretion and diffusion of FGF in microchambers

Using geometry of the actual device, we set up a finite element model combining growth factor secretion, diffusion and convection (COMSOL Inc., Los Angeles, CA). We assumed that 1) the population of resistant cells secrete FGF-2 with constant rate; 2) initial concentration of FGF-2 is negligible; and 3) convection within the microchannel is negligible. FGF-2 concentration profiles were obtained in two cases, blank hydrogel barrier and hydrogel barrier incorporating FGF-2 neutralizing antibodies. The values of parameters used in the simulation are summarized in Table 1. The initial antibody binding site density of FGF-2 was estimated by the concentration of antibodies embedded in a known volume of PEG hydrogel.

Table 1. Values of parameters used for modeling of FGF-2 secretion and diffusion

Diffusivity of FGF-2 in media at 37°C [29]	2.2×10^{-6} cm^2 s^{-1}
Diffusivity of FGF-2 in gel at 37°C (estimated) [30]	5.5×10^{-7} cm^2 s^{-1}
Initial antibody binding site density of FGF-2	2.6×10^{-6} mol L^{-1}
Association constant, K_{on} [31]	4.2×10^{2} μM^{-1} min^{-1}
Dissociation constant, K_{off} [31]	0.79 min^{-1}
Secretion rate of FGF-2 from resistant cells, R_{sec}	0.002759 pg cell^{-1} h^{-1}
Total number of resistant cells inside the channel	4,050

Inhibition of FGF and MEK signaling

In order to study the role of FGF in rescuing melanoma cells from death upon exposure to vemurafenib, we administered FGFR inhibitor (NVP-BGJ398, 0.2 μM). LOX-IMVI cells cultured in microchambers were simultaneously exposed to NVP-BGJ398 and 10 μm vemurafenib over a 48 h period. LOX-IMVI cells with either NVP-BGJ398 or vemurafenib were maintained inside microfluidic devices as controls. A similar procedure was followed for MEK inhibition experiments (PD0325901, 0.5 μM).

Incorporating FGF capture probes into gel barrier within a microfluidic device

Antibodies were covalently attached to PEG using protocols previously described.[32] Briefly, PEG-DA was first functionalized with N-hydroxysuccinimide (NHS) ester using NHS-PEG-acrylate and then incubated with Fc-FGFR1 molecules (100 μg/ml) for 1 h at RT. Photoinitiator solution was then added and the solution was infused into microfluidic chamber and the device was subsequently exposed to UV to form a gel.

RESULTS

Overview of the microfluidic co-culture experiment

The goal of this study was to test a hypothesis that paracrine signaling by FGF-2 in the tumor microenvironment contributes to vemurafenib resistance of adjacent non-FGF2-secreting *BRAF* mutant melanoma cells. To test this hypothesis we employed parental sensitive LOX-IMVI and A-375 cells and resistant LOX-IMVI-R melanoma cell lines which developed acquired resistance by an FGF-2 autocrine loop (Neve, unpublished). The cell lines were phenotypically indistinguishable except for resistance to vemurafenib; therefore, mixing of these cells had to be minimized. Furthermore, there was a requirement to selectively block FGF signaling in one group of cells in order to investigate response of the neighboring cells to drug treatment. To accomplish these goals, we fabricated microfluidic co-culture devices shown schematically in Fig. 1(A,B). These devices contained two cell culture compartments (length x width x height; 8 mm x 1.8 mm x 100 μm) each capable of housing ~5,000 cells. The compartments were separated by 100 μm wide PEG gel barrier (green lane in Fig.1A) that prevented physical interaction of cells and migration between compartments. Fig. 1C shows an image of the melanoma cells residing in parallel compartments separate by a channel filled with gel.

One of the primary objectives of this study was to discern paracrine effects independent of cell contact; hence it was important to build a platform with cells confined to specific locations on the culture surfaces. To test this, two groups of A-375 cells were labeled with either blue or green cell tracker dyes and infused into adjacent chambers. As shown in Fig. 1D, after 48 h of cultivation, blue and green cells remained

confined to their respective compartments. This confirmed that our microfluidic platform prevented intermixing of two groups of migratory cancer cells placed into close proximity over 48 h.

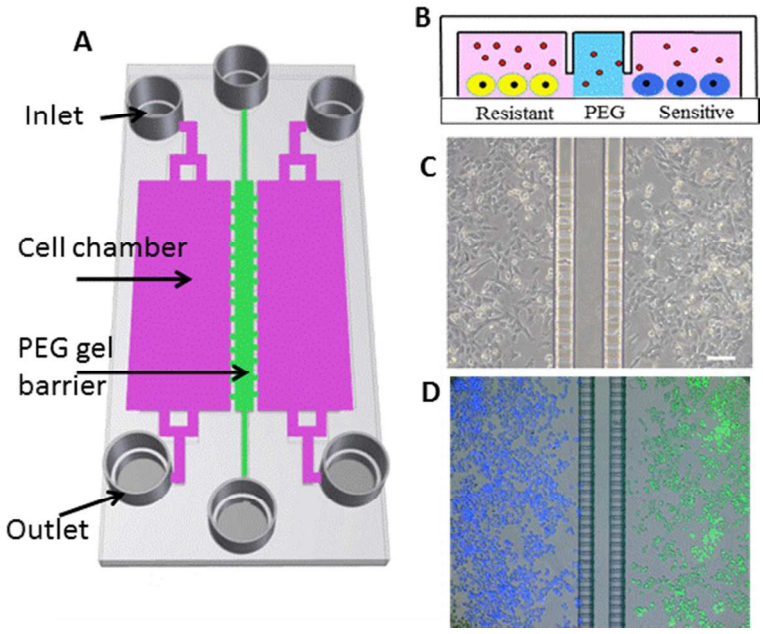

Fig. 1 A microfluidic co-culture device with semi-permeable PEG barrier. (A) Schematic of a device with two 1.8 mm-wide cell culture chambers in pink separated by a 100 µm PEG gel channel in green. (B) Cross-sectional view of two types of melanoma cells cultured in close proximity. (C) Brightfield image of A-375 cells cultured at Day 1. Scale bar represents 100µm. (D) A-375 cells were labeled with either green or blue cell-tracker dyers before being seeded in alternate chambers. Migration was assessed after a 48-h culture period..

The next set of experiments was designed to demonstrate diffusion of proteins through the gel barrier. Fluorescently labeled ovalbumin (MW 45 kDa) was used as a model paracrine signal in these experiments. Solution of this protein was infused into one cell compartment of the microfluidic device and was allowed to diffuse through the gel. As shown in Fig.2, fluorescent protein gradually diffused across the gel barrier so that after 18h there was no significant difference in fluorescence intensity. These findings highlight the fact that the gel channel separating cell compartments was permissive to diffusion of protein molecules of similar size scale to most of the paracrine signals of interest. In fact, at 17 kDa, FGF-2 is smaller than the ovalbumin-TRITC complex tested in Fig. 2.

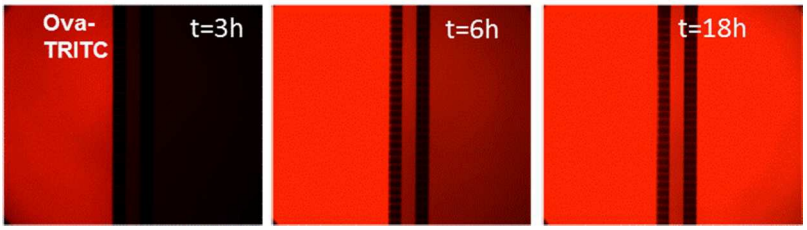

Fig. 2 Characterizing diffusion through PEG barrier. Fluorescently-labeled ovalbumin was infused in one chamber and its diffusion to the adjacent chamber was assessed over time.

Increased cell survival of LOX-IMVI melanoma cells in microchambers

The goal of the next set of experiments was to investigate drug responses of melanoma cells cultured alone inside microfluidic chambers. Originally, this was intended as a control experiment prior to co-cultivation sensitive cells with resistant cells, however, we observed that the normally sensitive melanoma cells (LOX-IMVI) cultured alone in microchambers became resistant to vemurafenib at high concentrations(20 μM) after 48 h inside microchambers (Fig. 3C). For comparison, in standard *in vitro* proliferation assays we found 0.1 μM vemurafenib caused significant cell death while 1 μM of this drug was associated with over 90% of cells dying (data not shown), which is consistent with published drug responses.[8, 33] This suggests that switching from sensitive to resistant phenotype was likely due to the microenvironment created inside the microfluidic device and not due to cell quality or another cell-related experimental artifact. It is also interesting to note that we have previously observed LOX-IMVI cells to become spontaneously resistant upon cultivation in 3D microenvironment (unpublished results). Therefore, there is precedent for culture-induced drug resistance in these cells.

Our lab has observed that other kinds of cells (stem cells and hepatocytes) cultured in microchambers without perfusion exhibited dramatically different phenotype compared to cells cultured under identical conditions in conventional culture plates. The reason for enhanced phenotype of these other cells was determined to be improved accumulation of endogenous GFs inside microchambers (unpublished data). We therefore hypothesized that similar effects could be taking place with LOX-IMVI cells. To test this hypothesis, LOX-IMVI and LOX-IMVI-R cells were seeded into 6-well plates and microchambers, and

then cultured for 48 h. ELISA analysis of culture media collected from these cells (Fig. 3D) revealed that LOX-IMVI and LOX-IMVI-R cells produced ~3- and 4-fold more FGF-2 respectively in microchambers compared to 6-well plates. As will be demonstrated later in this paper, the increase in FGF-2 production plays an important in survival of LOX-IMVI cells exposed to vemurafenib.

In contrast to LOX-IMVI cells, A-375 cells (another melanoma cell line) did not become resistant upon cultivation inside microchambers (Fig. S1). ELISA results revealed that A-375 cells produced measurably lower levels of FGF-2 compared LOX-IMVI cells (0.015 pg/cell vs. 0.07 pg/cell). These results strengthen the association of FGF-2 secretion with resistance to treatment with vemurafenib. Experiments in the next section demonstrate that inhibition of FGF-2 signaling abolishes resistance to vemurafenib in LOX-IMVI cells cultured in microchambers.

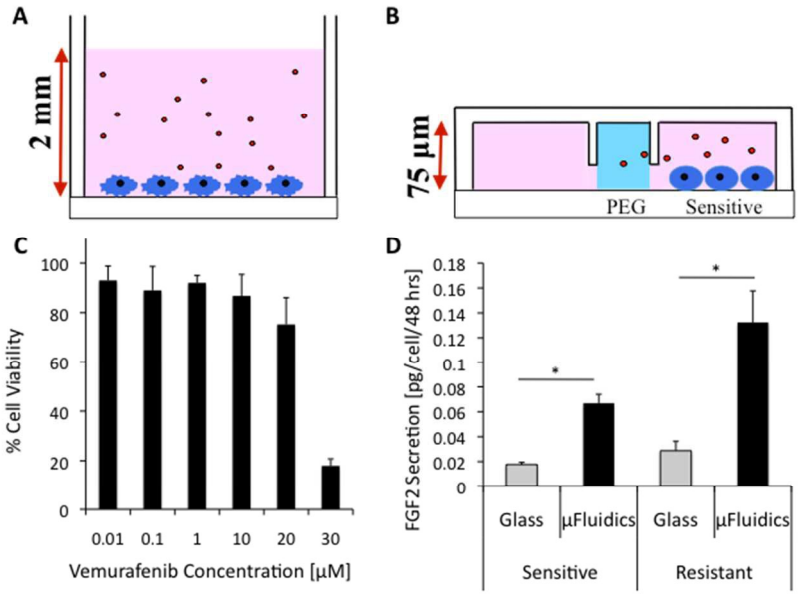

Fig. 3 Confinement of LOX-IMVI cells in microchambers leads to increased vemurafenib tolerance. (A,B) Schematics depicting cells bathed in vastly different amounts of media in (A) culture plate and (B) microchambers. (C) Dose-dependent response curve of LOX-IMVI cells to vemurafenib in microchambers. (D) FGF-2 ELISA measuring FGF-2 secretion in LOX-IMVI cells cultured in microchambers compared to culture plates. Results are represented as mean±SD (n=3). *: p-value < 0.05.

Mechanism of melanoma cell survival inside microchambers

Our next goal was to directly confirm that FGF-2 activation of FGFrs mediates drug resistance in LOX-IMVI cells cultured in microchambers. The cells were cultured in the presence of 0.2 μM NVP-BGJ398, a potent inhibitor of the FGF receptor (FGFR) [34, 35] (see Fig. 4A), and 10 μM vemurafenib. As shown in Fig.4B, in the absence of vemurafenib, 0.2 μM NVP-BGJ398 has no measurable effect on LOX-IMVI cell viability. However, the combination of 0.2 μM NVP-BGJ398 and 10 μM vemurafenib caused significant reduction in cell viability (Fig. 4B). This experiment demonstrates that FGF-2 / FGFR signaling is central to enhanced drug resistance inside microchambers.

We next explored which downstream survival pathway transduces FGF-2/FGFR mediated resistance in LOX-IMVI cells. We postulated that FGF-2 promoted reactivation of the MAPK pathway downstream of mutant BRAF (see Fig. 4A). Binding of ligand molecules to FGFR causes phosphorylation of receptor tyrosine kinase (RTK) with subsequent signal propagation occurring via phosphorylation of multiple downstream kinases including RAS, RAF and MEK. Of these kinases, MEK is a key target for shutting down MAPK signaling in melanoma (see Fig. 4A).[36-39] When LOX-IMVI cells were exposed to a combination of vemurafenib with MEK inhibitor inside microchambers we observed over 90% reduction in cell viability. This confirmed our hypothesis that FGF-2/FGFR signaling reactivated MAPK pathway downstream of BRAF and pointed to MEK as the possible site of this reactivation.

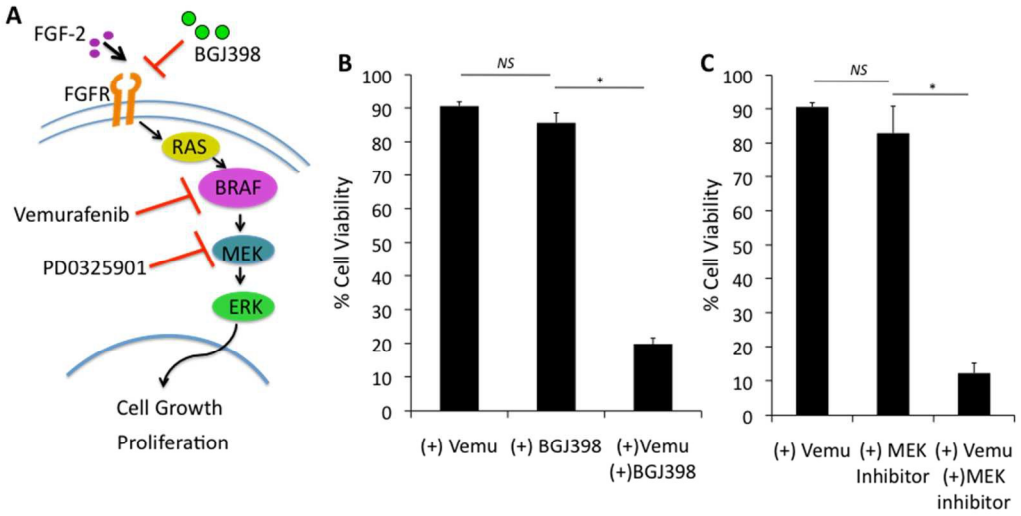

Fig. 4. Inhibition of components of MAPK pathway leads to cell death in microchambers. (A) Illustration of where FGF-2 inhibitors (NVP-BGJ298), vemurafenib and MEK inhibitors (PD0325901) act on the MAPK pathway. (B) Cell viability measurements of LOX-IMVI cells (B) in the presence of single and combined treatment with 0.2 nM NVP-BGJ398 and 10 μM vemurafenib, and (C) in the presence of single and combined treatment with 10 μM vemurafenib and 0.5 μM MEK inhibitor. Results are represented as mean±SD (n=3). *: p-value < 0.05. NS: Non-significant.

Paracrine signals confer resistance to melanoma cells in microfluidic chambers

Our initial intent was to co-culture resistant and sensitive LOX-IMVI cells inside the microfluidic chambers of the type shown in Fig.1 to test a hypothesis that FGF-2 secreted by resistant cells makes the cells in the adjacent compartment insensitive to vemurafenib. Since, LOX-IMVI cells became resistant when cultured inside microfluidic chambers; we utilized another melanoma cell line (A-375) which remained sensitive to vemurafenib in these chambers. A-375 cells cultured inside microchambers produced several fold less FGF-2 then LOX-IMVI and LOX-IMVI-R which is the likely reason why these cells remained sensitive. A-375 cells were co-cultured with LOX-IMVI-R cells to test effects of paracrine FGF-2 on drug resistance.

As shown schematically in Fig. 5(A), vemurafenib treatment of A-375 cultured alone inside microfluidic chambers caused significant inhibition of cell proliferation. We next tested the influence of LOX-IMVI-R cells, cultured in one compartment , on A-375 cell response to vemurafenib residing in an adjacent compartment. Fig. 5(A) highlights a dramatic protective effect of LOX-IMVI-R cells on A-375 cells in the presence of 10 μM vemurafenib. In monocultures of A-375 cells ~80% inhibition of cell proliferation was observed whereas in co-cultures with resistant cells only a 30% of cells lost proliferative capacity and viability in the presence of 10 μM of vemurafenib. These data provide compelling evidence of paracrine signal exchange being central to improved drug tolerance of A-375 cells. Based on the results shown in Fig.4, it was reasonable to presume that resistant cell-secreted factors, including FGF-2, that diffused to sensitive cells and triggered pro-survival signaling.

Interestingly, the effects of co-cultivation on drug resistance observed in microfluidic chambers could not be recapitulated by conditioned media experiments. Conditioned media from LOX-IMVI-R cells was

unable to prevent the reduction in cell viability of A-375 cells in the presence of 10 μM vemurafenib compared to control(see Fig.5B). This experiment suggests localized concentrations (paracrine) of growth factors exert very different effects compared to systemic (autocrine) secretion of the same factors, and highlights the advantages of microfluidic co-cultures in re-creating more *in vivo*-like high local concentrations of secreted factors.

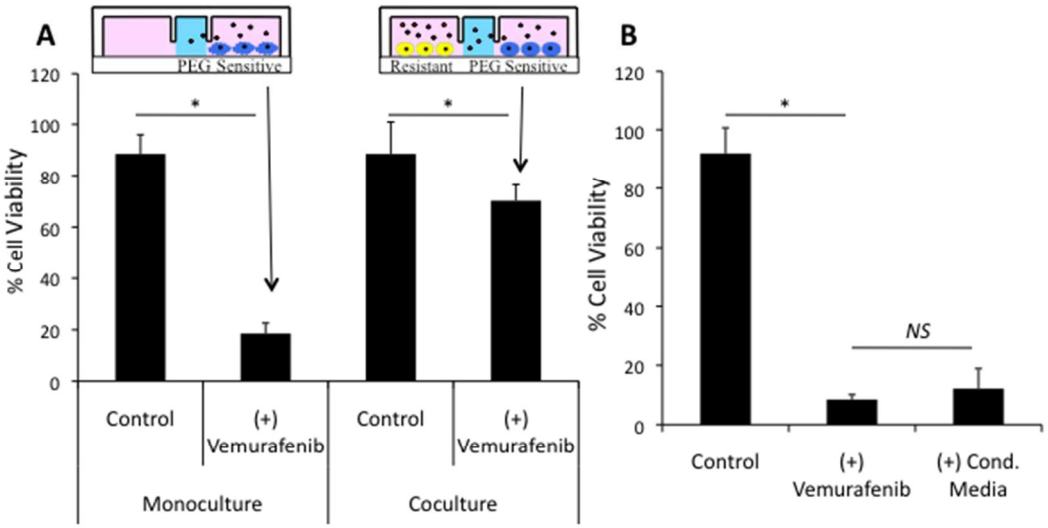

Fig. 5 Paracrine signals from LOX-IMVI-R cells rescue A-375 cells. (A) Effects of 10 μM venurafenib on A-375 cells in monoculture and in co-cultures with LOX-IMVI-R cells in microfluidic chambers. Schematics illustrate mono- and co-culture scenarios. (B) Effect of LOX-IMVI-R conditioned media on A-375 cell viability in standard cell cultures. Results are represented as mean±SD (n=3). *: p-value < 0.05. NS: Non-significant.

Modeling FGF-2 concentrations profiles inside a microfluidic device

ELISA was used to determine FGF-2 secretion rates for resistant and sensitive melanoma cells cultured inside microfluidic devices. A COMSOL model incorporating microchamber geometry, hydrogel barrier dimensions and diffusivity, as well as cell secretion rates was constructed into order to model FGF-2 concentration gradients inside the device. Secretion rates were assumed to be constant over time. Fig.6A shows evolution of FGF-2 concentration gradient over time in culture. As seen from modeling (Fig.6A,B), the concentration of FGF-2 in the sensitive cell compartment increased from ~1.5 nM at 12h to ~5 nM after 48h of cultivation. We tested whether concentrations of FGF-2 predicted by the model to be present inside the microfluidic chamber were sufficient to induce drug tolerance in sensitive melanoma

cells. To test this, A-375 cells were cultured in 96-well plates in media containing 1.5 nM FGF-2 and then exposed to varying concentrations of vemurafenib. Proliferation of cells was evaluated using MTT assay. As seen from Fig.6C, 1.5 nM of FGF-2 had a profound effect on proliferation and viability of A-375 cells. This suggests that FGF-2 secreted inside microfluidic device reached threshold concentrations affecting drug responsiveness as early as 12h into experiment. The results in Fig.6 also highlight the utility of modeling in defining parameters for testing drug resistance.

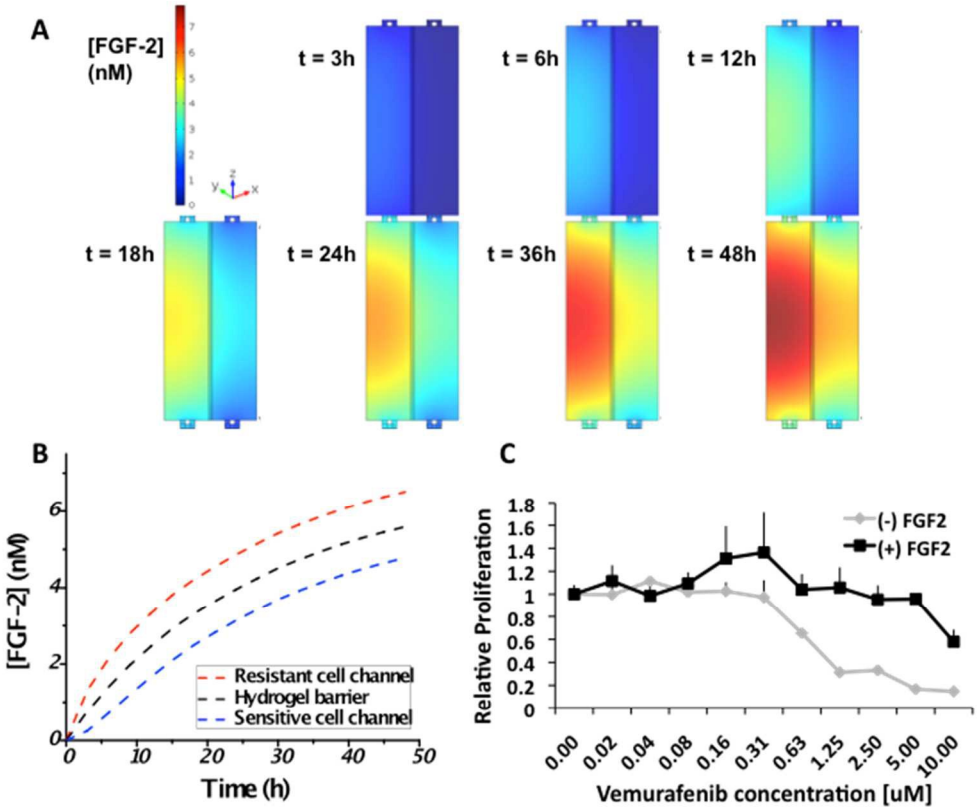

Fig. 6 Accumulation of FGF-2 in microchambers affects drug resistance properties of melanoma cells. (A) COMSOL simulation of FGF-2 secretion and diffusion in the microchambers as a function of time. Diffusion fields in microchambers show the distribution of FGF-2 secreted by the resistant cells. (B) Concentration profiles of FGF-2 across cell microchambers and hydrogel barrier over time were calculated. Secretion rates and other parameters relevant to modeling are described in Table 1. (C) MTT assay showing dose-dependent response of A-375 cells in a 96-well plate in the presence or absence of 1.5 nM FGF-2.

Selective interference of paracrine FGF-2 inside microfluidic devices

The preceding experiments clearly demonstrated that secreted FGF-2 plays a central role in inducing drug tolerance in melanoma cells. We wanted to conclusively prove that FGF-2 secreted by the resistant cells diffuses over and affects drug tolerance of neighboring sensitive cells. One strategy for proving this point may involve a knockdown or interference experiment whereby transcription or translation of FGF-2 is inhibited. However, a microfluidic co-culture system described here allowed for a different, arguably more holistic approach. In this approach, shown schematically in Fig. 7(A), the hydrogel barrier separating sensitive and resistant cells was loaded with FGF capture molecules - IgG fused with extracellular domain (ECD) of FGFR1 (Fc-FGFR chimera).[40] We constructed a COMSOL model of a scenario where hydrogel barrier actively scavenges/absorbs secreted FGF-2. This model accounted for the fact that the hydrogel was no longer a passive diffusion barrier but now included Fc-FGFR chimera that captured and retained FGF-2. Based on our estimation of the number of Abs loaded into the gel and secretory behavior of cells, very little FGF-2 was expected to diffuse over from resistant to sensitive cells residing in adjacent compartments (Fig. 7B and Fig.S2).

Interestingly, our model revealed that incorporation of Fc-FGFR chimeras into the gel not only prevented diffusion of this paracrine signal to sensitive cells but also decreased FGF-2 concentration in the resistant cell compartment (see Fig. 6B for blank gel and Fig. S2A for Ab-loaded gel device). This suggests that Fc-FGFR-carrying gel acted as a sink, absorbing secreted FGF-2 at a rate that exceeded simple diffusion. This discussion is quite relevant in light of results shown in Fig. 7C. First, drug tolerance of sensitive (A-375) cells was compromised in co-culture devices where FGF-2 secreted by resistant cells was captured in the gel. Over 70% of A-375 cells died after 48h exposure to vemurafenib in co-cultures containing FGF-2 trap in comparison to ~25% cell death in a co-culture device with blank gel. Second, drug tolerance of resistant melanoma cells (LOX-IMVI-R) was compromised in the microdevice with Ab-carrying gels (Fig. 7C). These cells became sensitive to vemurafenib, likely due to lower local concentration of autocrine FGF-2 predicted by modeling in Fig.7C. Our experiments and models

underscore the fact that secreted FGF-2-mediated drug resistance occurs through a combination of autocrine and paracrine signaling.

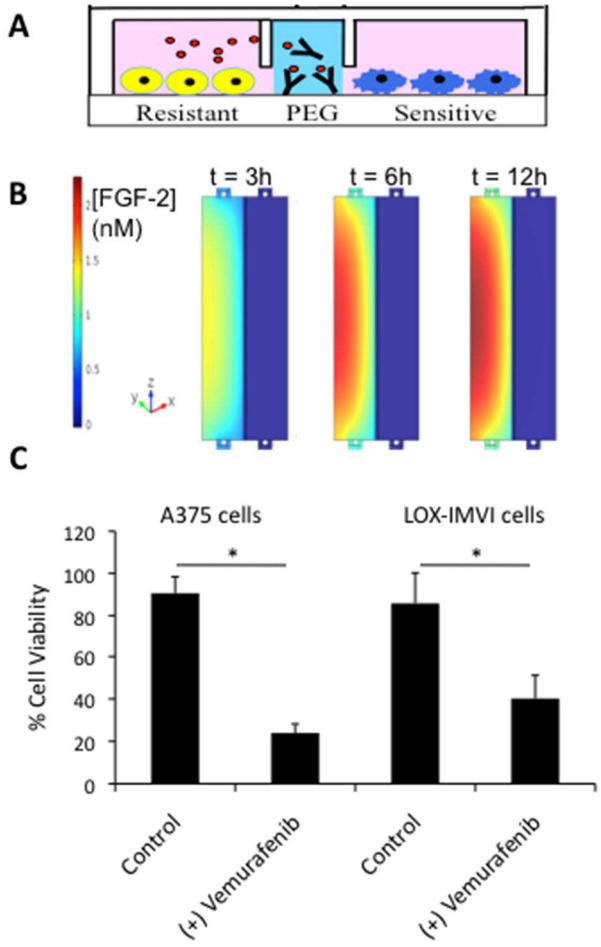

Fig. 7 Blocking FGF paracrine interactions between A-375 (sensitive) and LOX-IMVI-R (resistant) melanoma cells co-cultured inside a microfluidic device. (A) FGF neutralizing antibodies were incorporated into PEG gel separating cell compartments. (B) FGF-2 diffusion fields evaluated by COMSOL simulation in the presence of antibodies in the hydrogel barrier. (C) The effect of gel containing Fc-FGFR chimera on viability of LOX-IMVI-R and A-375 cells in the presence of 10 uM vemurafenib. Results are represented as mean±SD (n=3). *: p-value < 0.05. NS: Non-significant.

DISCUSSION

Targeted cancer therapies build on extensive research into molecular biology of cancers and represent more precise and nuanced approaches to cancer treatment. However, the promise of targeted therapies is undermined by drug resistance with patients becoming refractive to the drugs over time. This problem

affects both small molecule inhibitors targeting intracellular signaling elements (most often kinases) and monoclonal antibodies specific to cell-surface receptors. More and more evidence points to the milieu of signals in the cancer microenvironment playing an important role in activating alternative survival pathways and making cancer cells resistant to drugs shutting off primary pathways. Understanding the alternative survival pathways, the types of ligands triggering those pathways and the cell types secreting the ligands is important for establishing why resistance happens and for minimizing its effects. The questions listed above are best answered *in vitro* where cellular cross-talk and cell-specific signaling may be monitored with greater ease.

The goal of our study was to investigate how resistant melanoma cells confer drug resistance on sensitive melanoma cells. Specifically, we wanted to explore the role of FGF-2 in resistance to vemurafenib and the possibility that FGF-2 is produced by one group of cells (resistant to drug) and acts in a paracrine manner on neighboring sensitive cells. The choices available to us were: 1) transwell or conditioned media experiments, 2) pre-labeling of cells with different colors and mixing them in random co-cultures in standard cultureware or 3) utilizing a microfluidic co-culture platform that keeps the two groups of cancer cells separate but proximal. **Option 1** was eliminated early on. While we could induce resistance to vemurafenib by adding exogenous FGF-2 to sensitive melanoma cells (LOX-IMVI), we could not induce resistance with media conditioned by resistant cell line (LOX-IMVI-R). There were no easily identifiable morphological or surface marker differences between the two groups of melanoma cells with the exception of drug resistance. Therefore, mixing the two cell types at random for **Option 2** would have required labeling or engineering the two groups of cells to emit different fluorescence colors. While this strategy was feasible, we foresaw significant hurdles for any experiment beyond simple viability assessment. Cell type specific molecular biology analysis would have required sorting for desired cell types and would have limited our ability to work with viable cells. Therefore, microfluidic co-cultures (**Option 3**) were the obvious choice to study exchange of paracrine signals leading to cancer drug resistance.

The microfluidic device developed by us consisted of two parallel chambers separated by a thin gel barrier. This device was designed to place distinct groups of cells in close enough proximity to exchange paracrine signals while preventing resorting. One interesting and somewhat unexpected observation was switching of LOX-IMVI cells from sensitive to drug resistant phenotype upon cultivation inside our microfluidic device. We have seen phenotype enhancement in other cells (stem cells and liver cells) cultured in microfluidic devices and have connected changes in phenotype to accumulation of autocrine signals (Revzin, unpublished results). Similar to our previous observations, both sensitive and resistant LOX cell lines upregulated production of FGF-2 several fold inside the microfluidic chamber compared to standard 6-well plates. Given that our microfluidic devices are not perfused, secreted factors build up rapidly such that after 12 h in the microchamber, concentration of FGF-2 exceeds 2 nM (Fig. 6C) and is nearly 10 fold higher than in 6-well plates. Thus, FGF-2 accumulates inside microchambers, reaching threshold concentrations required to trigger survival signaling. As a side note, we have previously observed LOX cells become resistant to vemurafenib upon cultivation in 3D spheroids. In light of the fact that similar transition from sensitive to resistant phenotype was achieved in microfluidic cultures, it may be interesting to investigate, in the future, the role played by accumulation/transport of secreted signals in shaping phenotype of cancer cells in 3D microenvironment.

The key advantage of our platform was the ability to selectively eliminate a specific paracrine signal produced by a cell type of interest. Such an experiment is difficult to carry out using conventional cell culture tools but is straightforward to implement in our platform. FGF-2 secreted by resistant melanoma cells could be interfered with by immobilizing FGF-capture probes (Fc-FGFR1) into the hydrogel barrier separating the two compartments. This way, a specific secreted molecule could be eliminated from the milieu of signals produced by the cells of interest. In the future, we envision developing a medium- to high-throughput platform for investigating paracrine signals contributing to drug resistance of cancer cells.

It should be noted that in vitro cultures they have been shown to be useful for screening effectiveness of cancer drug therapies. In one example of such an assay, described by McMillin et al.,[41] in vitro co-cultures of cancer and stroma cells were found to be predictive of drug efficacy in vivo. A more recent study by Straussman et al. demonstrated that stromal production of HGF correlated with drug resistance of BRAF mutant melanoma cell lines in vitro as well as with drug resistance in patients.[12] These and other findings suggest that; while reductionist and simplistic, in vitro cultures may be used to predict drug effectiveness in vivo.

CONCLUSION

The goal of this study was to investigate the role played by FGF-2 as a mediator of drug resistance in *BRAF* mutant melanoma cells. To test the hypothesis that FGF-2 was a paracrine signal produced by the resistant cells in the cancer microenvironment, we developed a microfluidic co-culture system that physically separated migratory melanoma cell lines while permitting exchange of paracrine signals. This microfluidic device was used to demonstrate that FGF-2 acted in both paracrine and autocrine manner in our microfluidic devices. Autocrine signaling drove previously sensitive melanoma cells to become tolerant to vemurafenib. Paracrine signals were eliminated by incorporating FGF capture probes into the gel barrier separating resistant and sensitive cells. Interference with paracrine FGF-2 signaling broke tolerance of sensitive melanoma cells to vemurafenib.

The tumor cell microenvironment created inside a microfluidic chamber may be a better mimic of distances and local concentrations present *in vivo.* Our microfluidic platform also includes a hydrogel barrier that may be converted into a ligand trap by incorporating capture probes specific to a paracrine signal of interest. Furthermore, these miniaturized cell culture platforms require just a few thousand cells and may in the future be used to determine patient-specific drug resistance profiles for personalized cancer therapies.

ACKNOWLEDGEMENTS

Authors acknowledge financial support from NSF (1233617 and 1403561). Additional funding came from "Research Investment in Science and Engineering" project at UC Davis.

References

1. S. Jang and M. B. Atkins, *Clinical pharmacology and therapeutics*, 2014, **95**, 24-31.
2. G. Bollag, P. Hirth, J. Tsai, J. Zhang, P. N. Ibrahim, H. Cho, W. Spevak, C. Zhang, Y. Zhang, G. Habets, E. A. Burton, B. Wong, G. Tsang, B. L. West, B. Powell, R. Shellooe, A. Marimuthu, H. Nguyen, K. Y. Zhang, D. R. Artis, J. Schlessinger, F. Su, B. Higgins, R. Iyer, K. D'Andrea, A. Koehler, M. Stumm, P. S. Lin, R. J. Lee, J. Grippo, I. Puzanov, K. B. Kim, A. Ribas, G. A. McArthur, J. A. Sosman, P. B. Chapman, K. T. Flaherty, X. Xu, K. L. Nathanson and K. Nolop, *Nature*, 2010, **467**, 596-599.
3. J. T. Lee, L. Li, P. A. Brafford, M. van den Eijnden, M. B. Halloran, K. Sproesser, N. K. Haass, K. S. Smalley, J. Tsai, G. Bollag and M. Herlyn, *Pigment cell & melanoma research*, 2010, **23**, 820-827.
4. P. B. Chapman, A. Hauschild, C. Robert, J. B. Haanen, P. Ascierto, J. Larkin, R. Dummer, C. Garbe, A. Testori, M. Maio, D. Hogg, P. Lorigan, C. Lebbe, T. Jouary, D. Schadendorf, A. Ribas, S. J. O'Day, J. A. Sosman, J. M. Kirkwood, A. M. Eggermont, B. Dreno, K. Nolop, J. Li, B. Nelson, J. Hou, R. J. Lee, K. T. Flaherty and G. A. McArthur, *The New England journal of medicine*, 2011, **364**, 2507-2516.
5. K. T. Flaherty, I. Puzanov, K. B. Kim, A. Ribas, G. A. McArthur, J. A. Sosman, P. J. O'Dwyer, R. J. Lee, J. F. Grippo, K. Nolop and P. B. Chapman, *The New England journal of medicine*, 2010, **363**, 809-819.
6. J. A. Sosman, K. B. Kim, L. Schuchter, R. Gonzalez, A. C. Pavlick, J. S. Weber, G. A. McArthur, T. E. Hutson, S. J. Moschos, K. T. Flaherty, P. Hersey, R. Kefford, D. Lawrence, I. Puzanov, K. D. Lewis, R. K. Amaravadi, B. Chmielowski, H. J. Lawrence,

Y. Shyr, F. Ye, J. Li, K. B. Nolop, R. J. Lee, A. K. Joe and A. Ribas, *The New England journal of medicine*, 2012, **366**, 707-714.

7. M. R. Lackner, T. R. Wilson and J. Settleman, *Future Oncol.*, 2012, **8**, 999-1014.
8. T. R. Wilson, J. Fridlyand, Y. B. Yan, E. Penuel, L. Burton, E. Chan, J. Peng, E. Lin, Y. L. Wang, J. Sosman, A. Ribas, J. Li, J. Moffat, D. P. Sutherlin, H. Koeppen, M. Merchant, R. Neve and J. Settleman, *Nature*, 2012, **487**, 505-U1652.
9. O. Casanovas, D. J. Hicklin, G. Bergers and D. Hanahan, *Cancer Cell*, 2005, **8**, 299-309.
10. J. M. Llovet and A. Villanueva, *Clin Cancer Res*, 2012, **doi: 10.1158/1078-0432**.
11. D. B. Hoelzinger, T. Demuth and M. E. Berens, *Journal of the National Cancer Institute*, 2007, **99**, 1583-1593.
12. R. Straussman, T. Morikawa, K. Shee, M. Barzily-Rokni, Z. R. Qian, J. Y. Du, A. Davis, M. M. Mongare, J. Gould, D. T. Frederick, Z. A. Cooper, P. B. Chapman, D. B. Solit, A. Ribas, R. S. Lo, K. T. Flaherty, S. Ogino, J. A. Wargo and T. R. Golub, *Nature*, 2012, **487**, 500-U118.
13. L. A. Diaz, Jr., R. T. Williams, J. Wu, I. Kinde, J. R. Hecht, J. Berlin, B. Allen, I. Bozic, J. G. Reiter, M. A. Nowak, K. W. Kinzler, K. S. Oliner and B. Vogelstein, *Nature*, 2012, **486**, 537-540.
14. H. Shi, W. Hugo, X. Kong, A. Hong, R. C. Koya, G. Moriceau, T. Chodon, R. Guo, D. B. Johnson, K. B. Dahlman, M. C. Kelley, R. F. Kefford, B. Chmielowski, J. A. Glaspy, J. A. Sosman, N. van Baren, G. V. Long, A. Ribas and R. S. Lo, *Cancer discovery*, 2014, **4**, 80-93.
15. A. C. Obenauf, Y. Zou, A. L. Ji, S. Vanharanta, W. Shu, H. Shi, X. Kong, M. C. Bosenberg, T. Wiesner and N. Rosen, *Nature*, 2015.

16. M. Katoh and H. Nakagama, *Medicinal research reviews*, 2014, **34**, 280-300.

17. G. Lefevre, N. Babchia, A. Calipel, F. Mouriaux, A. M. Faussat, S. Mrzyk and F. Mascarelli, *Investigative ophthalmology & visual science*, 2009, **50**, 1047-1057.

18. K. E. Ware, T. K. Hinz, E. Kleczko, K. R. Singleton, L. A. Marek, B. A. Helfrich, C. T. Cummings, D. K. Graham, D. Astling, A. C. Tan and L. E. Heasley, *Oncogenesis*, 2013, **2**, e39.

19. F. Liu, J. Cao, J. Wu, K. Sullivan, J. Shen, B. Ryu, Z. Xu, W. Wei and R. Cui, *The Journal of investigative dermatology*, 2013, **133**, 2041-2049.

20. M. Domenech, H. Yu, J. Warrick, N. M. Badders, I. Meyvantsson, C. M. Alexander and D. J. Beebe, *Integrative biology : quantitative biosciences from nano to macro*, 2009, **1**, 267-274.

21. S. N. Bhatia, M. L. Yarmush and M. Toner, *J. Biomed. Mater. Res.*, 1997, **34**, 189-199.

22. J. Y. Lee, N. Tuleuova, C. N. Jones, E. Ramanculov, M. A. Zern and A. Revzin, *Integrative Biology*, 2009, **1**, 460-468.

23. G. S. Stybayeva, H. Zhu, E. Ramanculov, S. Dandekar, M. D. George and A. Revzin, *Biochem. Biophys. Res. Commun.*, 2009, **380**, 575-580.

24. S. N. Bhatia, U. J. Balis, M. L. Yarmush and M. Toner, *Biotechnol. Prog.*, 1998, **14**, 378-387.

25. Y. D. Gao, D. Majumdar, B. Jovanovic, C. Shaifer, P. C. Lin, A. Zijlstra, D. J. Webb and D. Y. Li, *Biomedical microdevices*, 2011, **13**, 539-548.

26. D. Majumdar, Y. D. Gao, D. Y. Li and D. J. Webb, *Journal of neuroscience methods*, 2011, **196**, 38-44.

27. T. Kwa, Q. Zhou, Y. Gao, A. Rahimian, L. Kwon, Y. Liu and A. Revzin, *Lab on a Chip*, 2014, **14**, 1695-1704.

28. D. Patel, A. Haque, Y. Gao and A. Revzin, *Integrative Biology*, 2015, **7**, 815-824.

29. M. T. Tyn and T. W. Gusek, *Biotechnology and bioengineering*, 1990, **35**, 327-338.

30. B. Amsden, *Macromolecules*, 1998, **31**, 8382-8395.

31. R. J. Filion and A. S. Popel, *Annals of biomedical engineering*, 2004, **32**, 645-663.

32. D. S. Shin, J. You, A. Rahimian, T. Vu, C. Siltanen, A. Ehsanipour, G. Stybayeva, J. Sutcliffe and A. Revzin, *Angewandte Chemie (International ed. in English)*, 2014, **53**, 8221-8224.

33. H. Yang, B. Higgins, K. Kolinsky, K. Packman, Z. Go, R. Iyer, S. Kolis, S. Zhao, R. Lee, J. F. Grippo, K. Schostack, M. E. Simcox, D. Heimbrook, G. Bollag and F. Su, *Cancer research*, 2010, **70**, 5518-5527.

34. E. Nummenmaa, M. Hamalainen, T. Moilanen, K. Vuolteenaho and E. Moilanen, *Scandinavian journal of rheumatology*, 2015, DOI: 10.3109/03009742.2014.1000372, 1-10.

35. T. Garay, E. Molnar, E. Juhasz, V. Laszlo, T. Barbai, J. Dobos, K. Schelch, C. Pirker, M. Grusch, W. Berger, J. Timar and B. Hegedus, *Pathology oncology research : POR*, 2015, DOI: 10.1007/s12253-015-9916-9.

36. K. T. Flaherty, C. Robert, P. Hersey, P. Nathan, C. Garbe, M. Milhem, L. V. Demidov, J. C. Hassel, P. Rutkowski, P. Mohr, R. Dummer, U. Trefzer, J. M. Larkin, J. Utikal, B. Dreno, M. Nyakas, M. R. Middleton, J. C. Becker, M. Casey, L. J. Sherman, F. S. Wu, D. Ouellet, A. M. Martin, K. Patel and D. Schadendorf, *The New England journal of medicine*, 2012, **367**, 107-114.

37. A. M. Grimaldi, E. Simeone and P. A. Ascierto, *Current opinion in oncology*, 2014, **26**, 196-203.

38. D. B. Solit, L. A. Garraway, C. A. Pratilas, A. Sawai, G. Getz, A. Basso, Q. Ye, J. M. Lobo, Y. She, I. Osman, T. R. Golub, J. Sebolt-Leopold, W. R. Sellers and N. Rosen, *Nature*, 2006, **439**, 358-362.

39. R. J. Sullivan and K. Flaherty, *Oncogene*, 2013, **32**, 2373-2379.

40. A. Sokolowska-Wedzina, A. Borek, J. Chudzian, P. Jakimowicz, M. Zakrzewska and J. Otlewski, *Protein expression and purification*, 2014, **99**, 50-57.

41. D. W. McMillin, J. Delmore, E. Weisberg, J. M. Negri, D. C. Geer, S. Klippel, N. Mitsiades, R. L. Schlossman, N. C. Munshi, A. L. Kung, J. D. Griffin, P. G. Richardson, K. C. Anderson and C. S. Mitsiades, *Nat. Med.*, 2010, **16**, 483-U171.